

MICROSTRUCTURAL CHARACTERIZATION OF PRIMARY COOLANT PIPE STEEL

M.K. Miller and J. Bentley

CONF-860752--1

Metals and Ceramics Division
Oak Ridge National Laboratory
Oak Ridge, TN 37831, USA

DE86 012631

By acceptance of this article, the
publisher or recipient acknowledges
the U.S. Government's right to
retain a nonexclusive, royalty-free
license in and to any copyright
covering the article.

MASTER

Abstract - Atom probe field-ion microscopy, analytical electron microscopy, and optical microscopy have been used to investigate the changes that occur in the microstructure of cast CF 8 primary coolant pipe stainless steel after long term thermal aging. The cast duplex microstructure consisted of austenite with 15% δ -ferrite. Investigation of the aged material revealed that the ferrite spinodally decomposed into a fine scaled network of α and α' . A fine G-phase precipitate was also observed in the ferrite. The observed degradation in mechanical properties is probably a consequence of the spinodal decomposition in the ferrite.

INTRODUCTION

The mechanical properties of the cast stainless steel pipes that are used to carry the primary coolant water in pressurized water nuclear reactors are known to be degraded by exposure to elevated temperatures in the range 300 to 400°C. The cast stainless steel used for these pipes forms a duplex microstructure of austenite and ferrite. The ferrite increases the yield strength of the cast material and also reduces the susceptibility to hot cracking during solidification. However, long term thermal aging produces an increase in hardness and tensile properties, together with a decrease in the impact properties, ductility, and toughness.

A previous combined atom probe field-ion microscopy (APFIM) and analytical electron microscopy (AEM) investigation of a duplex CF 8M alloy indicated that two phase transformations had occurred during aging which could contribute to the changes in mechanical properties [1]. The ferrite, after aging for 7500 h at 400°C, had spinodally decomposed to form an interconnected network of iron-rich α phase and chromium-enriched α' phase. The precipitation of a G-phase nickel silicide was also observed in the ferrite. It was suggested that small changes in the composition of the alloy could affect the quantities of the phases present by altering the position of the miscibility gap or by suppressing the formation of G-phase [1].

In this paper, the microstructure present after extended thermal aging of a cast CF 8 stainless steel, a variant of the previous steel with a lower molybdenum content, will be presented and compared to the previously reported results. The techniques of atom probe field-ion microscopy, analytical electron microscopy, and optical microscopy were used to characterize the microstructure.

Chopra and Chung showed that a CF 8 stainless steel, (heat 278), suffered a dramatic loss in impact properties, dropping to almost 15% of the initial value after prolonged aging [2]. Some microstructural characterization of several heats of CF 8 and other similar stainless steels was also presented by these authors [2,3].

EXPERIMENTAL

The stainless steel used in this investigation was a cast CF 8 alloy (heat 278) from

Georg Fischer Co. of Switzerland. The nominal compositions of this alloy [2] and the previously examined CF 8M alloy [1] are given in Table 1. The CF 8 steel was examined after laboratory aging for 70,000 h at 300, 350 or 400°C. The APFIM analyses were conducted on the ORNL atom probe [4]. The AEM analyses were performed on Philips EM400T/FEG and EM430T analytical electron microscopes both equipped with EDAX 9100/70 energy dispersive X-ray spectrometer (EDS) and Gatan 607 electron energy loss spectrometer (EELS) systems.

Table 1. Nominal composition of the CF 8 and CF 8M steels (wt%).

Alloy	Cr	Ni	Si	Mn	Mo	C	N	S	P	Fe
CF 8	20.2	8.3	1.0	0.28	0.13	0.038	0.027	0.019	0.008	balance
CF 8M	20.8	10.6	0.81	0.79	2.5	0.04	0.042	0.021	0.016	balance

RESULTS

Optical microscopy indicated that the cast and aged materials consisted of a duplex microstructure of austenite with approximately 15% ferrite, in agreement with the calculated value of 19% [2]. A comparison of the duplex microstructure of the materials aged at 300 and 400°C is shown in the the electron micrographs in figure 1. In the material aged at 400°C the ferrite had undergone a small amount of reversion to austenite at the ferrite-austenite interface, to a depth of approximately 4 μm , with the precipitation of some carbides, figure 1b. Most of these precipitates were preferentially located at the original ferrite-austenite interface. Analysis of these precipitates by AEM and APFIM revealed that they were chromium-rich M_{23}C_6 carbides. No carbides or reversion of the ferrite were observed in the materials aged at 300°C, figure 1a. The ferrite had slightly reverted in the material aged at 350°C, but no carbides were observed.

The microhardness of the ferrite was found to increase on aging, whereas the microhardness of the austenite did not change significantly. Analyses of the compositions of the ferrite and austenite by energy dispersive X-ray spectroscopy revealed that the ferrite was enriched in chromium, silicon, and molybdenum and depleted in nickel and manganese as shown in Table 2.

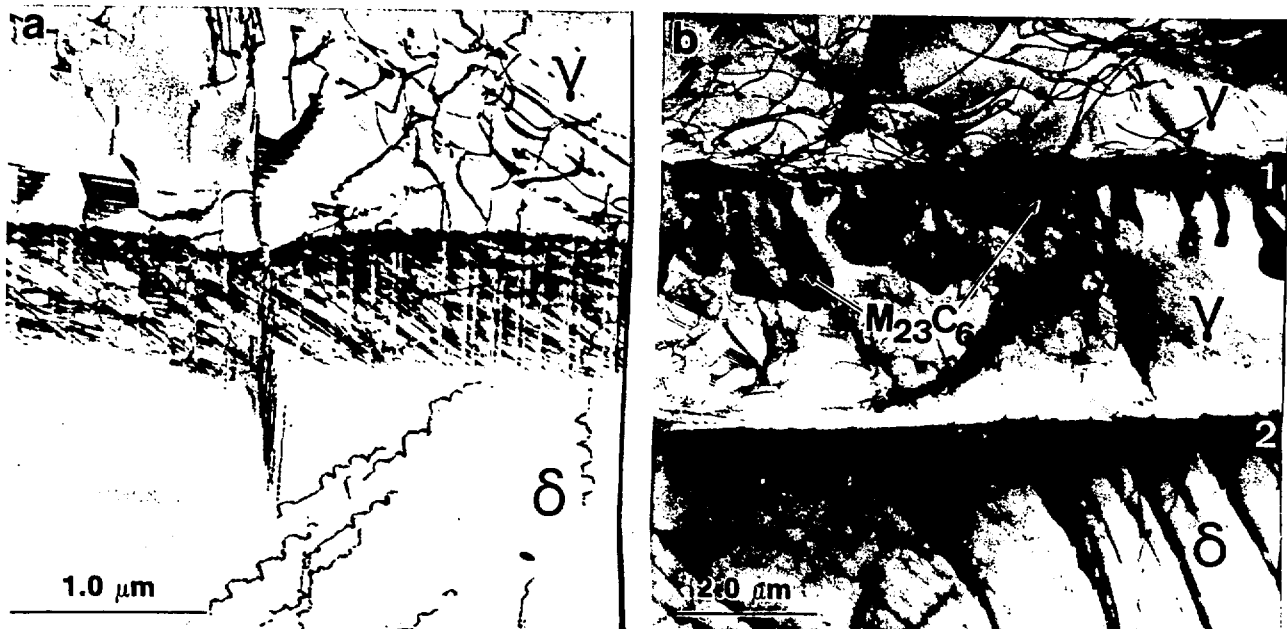


Fig.1. AEM characterization of the microstructure of cast CF 8 stainless steel. The δ -ferrite reverts to austenite, Y, and M_{23}C_6 at 400°C but not at 300°C. The original ferrite-austenite interface is at position 1.

Table 2. EDS analysis of the compositions of austenite and ferrite after aging for 70000 h at 400°C (wt%).

	Austenite	Ferrite
Chromium	20.2	28.6
Nickel	8.4	3.7
Manganese	0.22	0.08
Molybdenum	0.26	0.36
Silicon	0.99	1.42
Iron	Balance	Balance

More detailed analyses of the ferrite by AEM and APPIM revealed that it had decomposed during aging. Electron micrographs of the structure in material aged at 300 and 400°C are shown in figure 2. The scale of this two phase modulated microstructure was measured from these electron micrographs as 4 and 9 nm in the 300 and 400°C aged materials, respectively. A field-ion micrograph of the same two phase microstructure in the 400°C aged material is shown in figure 3, where the darkly imaging α' and the brightly imaging α phases are evident. The periodicity of the modulations of the two phases was measured from FIM micrographs to be 7 nm. Field evaporation sequences also revealed that the modulated microstructure was interconnected in three dimensions, indicative of phase separation by isotropic spinodal decomposition. An atom probe composition profile through the ferrite, figure 4, also indicates that the ferrite had decomposed into a chromium-enriched α' phase and an iron-rich α phase.

AEM also indicated the presence of some very fine precipitates in the ferrite as shown in figure 5. These precipitates were identified as G-phase from their cube-on-cube orientation relationship with the ferrite, the face centered cubic structure (Fm3m space group), the lattice parameter of 1.11 nm, and the absence of the 400 reflection [1,5].

In both 300 and 400°C aged materials, distinct bimodal size distributions of the G-phase precipitates were observed. The smaller precipitates were randomly distributed in the ferrite matrix, whereas the larger precipitates were associated with dislocations. This is illustrated in figure 6 which shows G-phase precipitates imaged in dark field with a precipitate reflection, dislocations imaged under weak beam dark field conditions, and a superposition of these images.

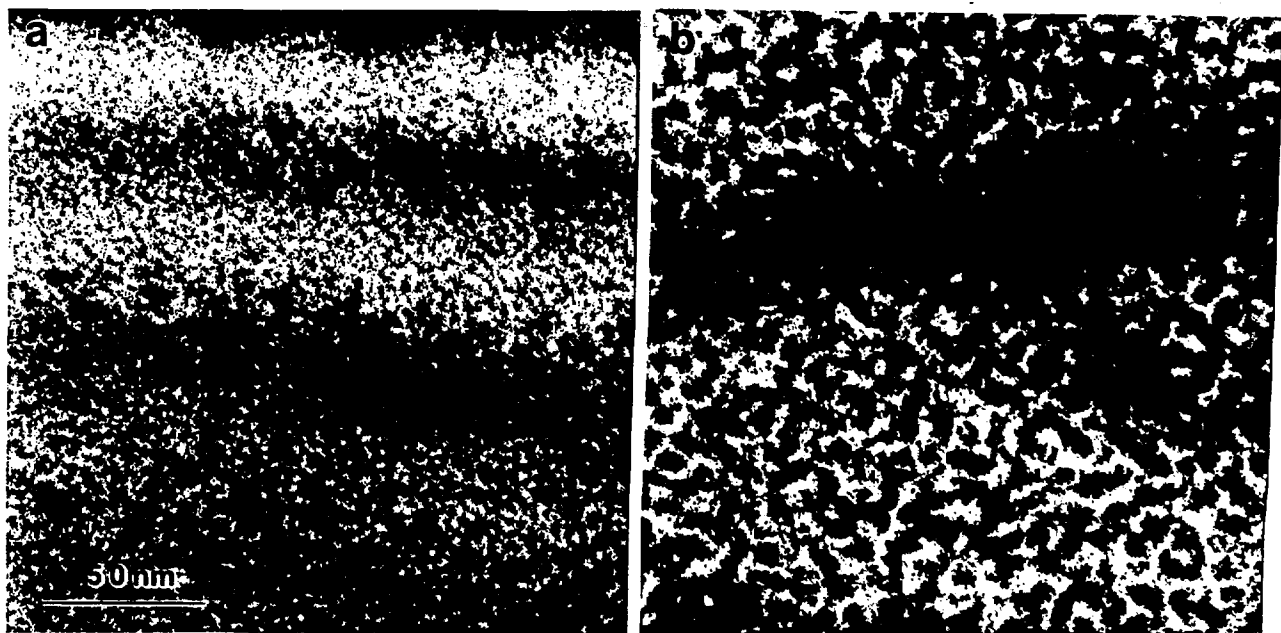


Fig. 2. Electron micrographs of the ferrite in CF 8 stainless steel showing isotropic spinodal decomposition in the materials aged for 70000 h at 300 and 400°C.



Fig. 3. Field-ion micrograph of the ferrite in the 400°C aged alloy showing darkly imaging α' and brightly imaging α .

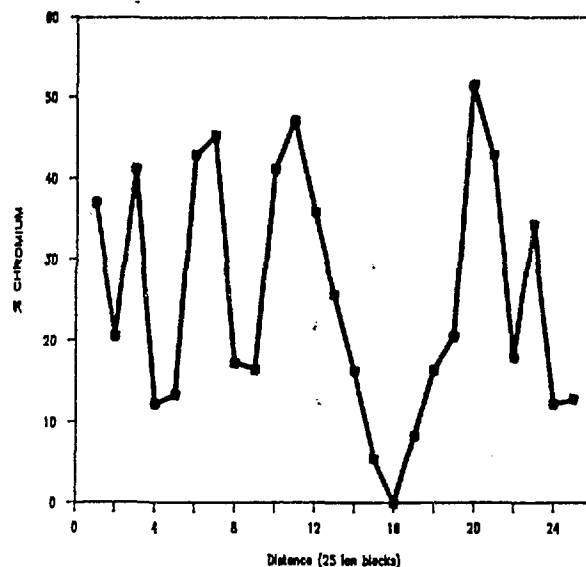


Fig. 4. Atom probe composition profile through the ferrite in the 400°C aged steel chromium-enriched α' and iron-rich α phases.

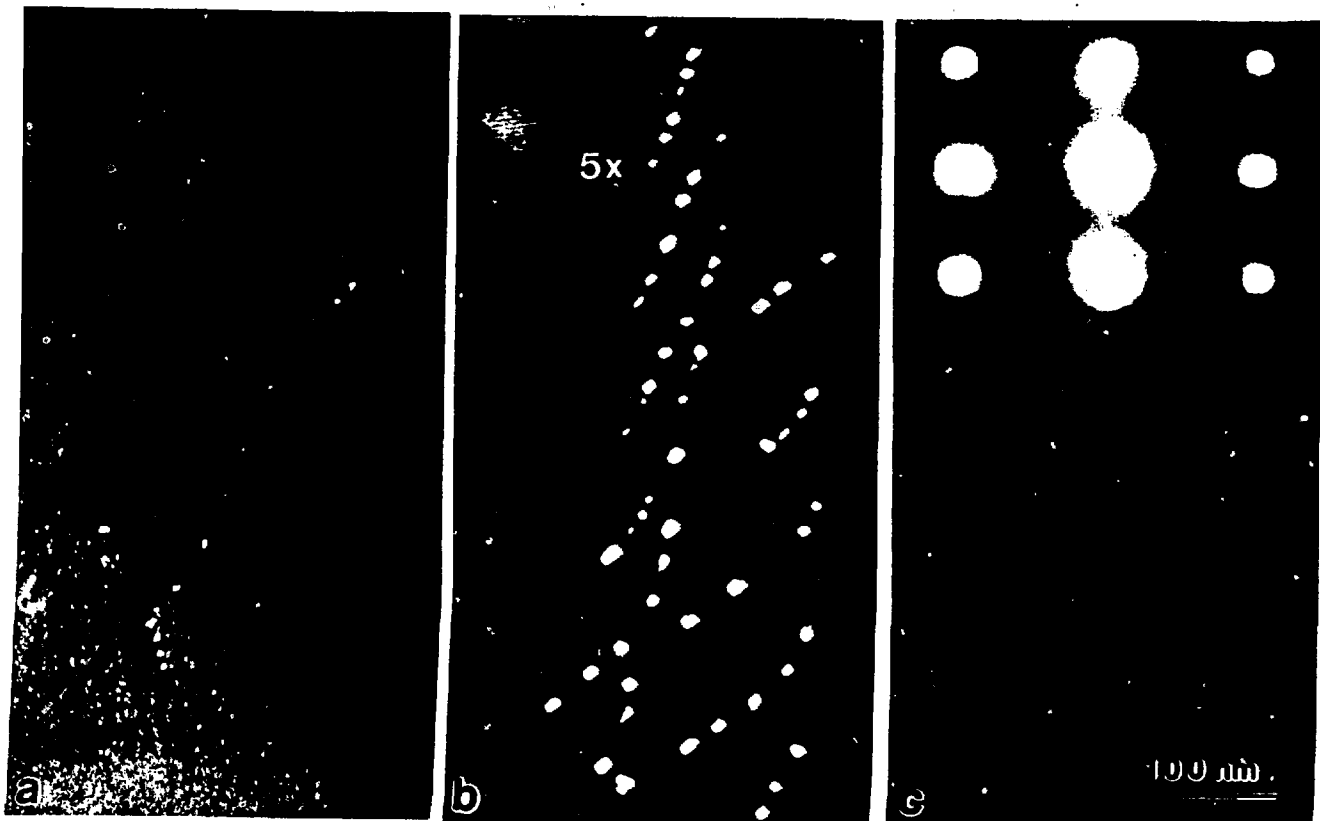


Fig. 5. Dark field electron micrographs of the CF 8 steel showing G-phase precipitates, (a) in material aged at 300°C, (b) on dislocations in material aged at 400°C, and (c) in the matrix in material aged at 400°C. Inset in (b) shows fine fringes present on the precipitates and the inset in (c) shows a 110 oriented diffraction pattern from these precipitates. The larger precipitates were associated with dislocations in both aged materials.

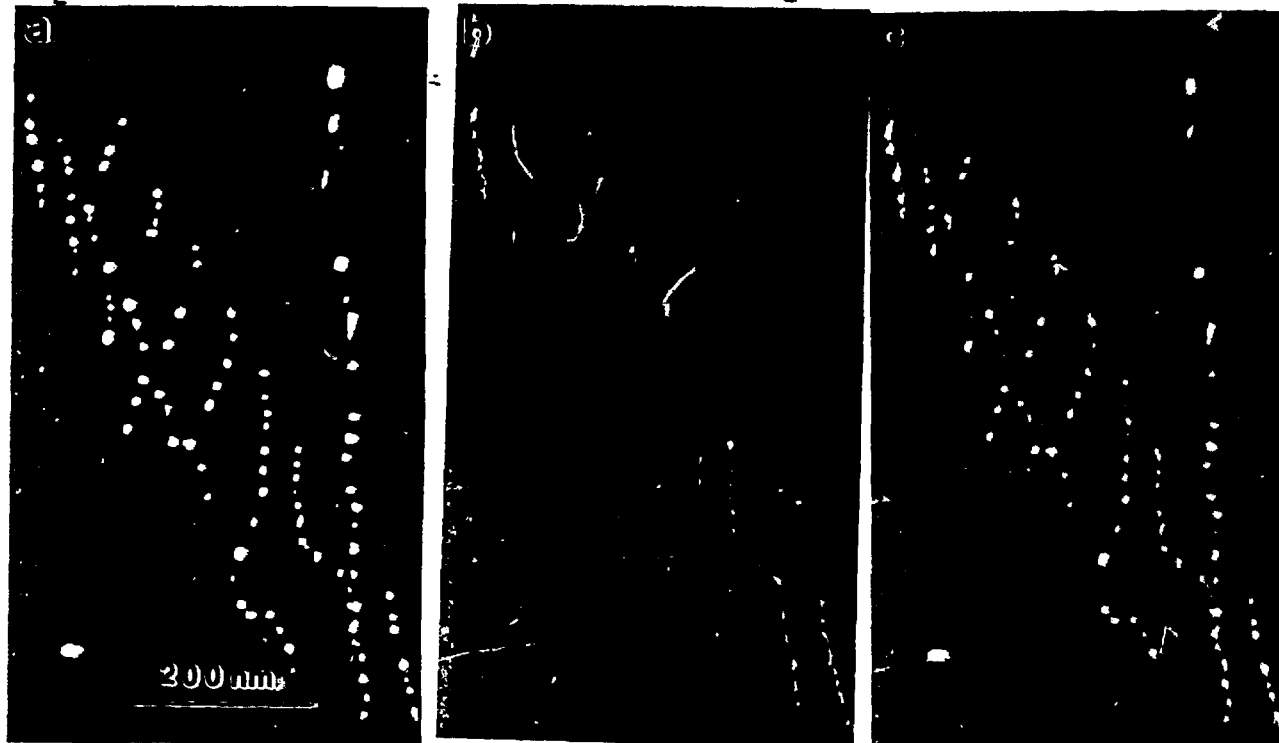


Fig. 6. Electron micrographs of the 400°C aged CF 8 steel showing the coarser G-phase precipitates associated with dislocations, (a) precipitate dark field, (b) weak beam dark field, and (c) superposition of (a) and (b).

The finer precipitates were approximately 1.5 and 2 nm in diameter in the materials aged at 300 and 400°C, respectively. In both aged materials, the particles were 4 to 5 times larger on the dislocations than in the matrix, presumably due to enhanced nucleation and growth because of assistance of pipe diffusion along the dislocation core.²¹ The number density of these G-phase precipitates was $>10^{24}$ and approximately 10^{21} m^{-3} in the 300 and 400°C aged material respectively. It should be emphasized that the G-phase would have been overlooked due to its small size and limited contribution to the electron diffraction patterns without the previous characterization of the CF 8M steel.

DISCUSSION

The results of this investigation of the CF 8 steel were similar to those reported previously for the CF 8M alloy. In both types of steel the ferrite spinodally decomposed into an isotropic network of α and α' phases and G-phase precipitated. The major difference between the two types of steels was the size and number density of the G-phase precipitates. In the CF 8M material aged 7500 h at 400°C the G-phase precipitates were much larger, ~10 nm in diameter, and were present at a much larger number density, $\sim 10^{23} \text{ m}^{-3}$, compared to the CF 8 that was also aged at 400°C but for almost 10 times longer. This larger volume of G-phase is related to the differences in initial composition between the two alloys. The G-phase silicide is rich in nickel and molybdenum [1,5,6] which had higher levels in the CF 8M steel than the CF 8 steel, Table 1.

While a small fraction of the G-phase precipitates were observed pinning the dislocations, it should be noted that these residual dislocations will not necessarily be of the same type, or behave in the same manner, as those generated during shock loading. G-Phase precipitates on dislocations in ferrite has been previously observed by Vitek in similar steels [7].

The fine scale spinodal decomposition and the G-phase precipitation in the ferrite both contribute to the changes in mechanical properties that occur during aging. However, since the volume of the G-phase was lower than that observed in the CF 8M

steel the degradation in mechanical properties is primarily due to the spinodal decomposition that occurs in the ferrite during aging. In addition, the observation that the increase in hardness in the CF 8 and CF 8M steels is similar to that previously observed in a spinodally decomposed iron - 30% chromium alloy which did not contain any G-phase [8], also suggests that spinodal decomposition is the primary factor influencing mechanical properties.

Finally, it should also be noted that conclusions drawn from the results of accelerated tests that are usually performed at 400°C [9] should be carefully examined since the microstructures that develop are not identical to those at 300°C. This difference in the microstructure was indicated by the reversion of the ferrite into austenite and the precipitation of $M_{23}C_6$ that occurred at 400°C but not at the lower temperatures of 350 or 300°C. The presence of these carbides could then be a factor in the fracture process and thereby alter the mechanical properties.

SUMMARY

Both APFIM and AEM results indicate that the chromium-enriched ferrite had decomposed into a very fine network of chromium-enriched α' and iron-rich α phases as a result of isotropic spinodal decomposition. A coarse $M_{23}C_6$ precipitate was observed at the ferrite-austenite interface in the material that was aged at 400°C. Very fine G-phase silicide precipitates were observed in the ferrite. A comparison between the results from this CF 8 alloy and the previously reported results of a CF 8M alloy indicates that relatively small differences in the alloy compositions significantly alter the quantity of phases present in the microstructure. The degradation in mechanical properties is probably a consequence of the spinodal decomposition of the ferrite that occurs during aging.

Acknowledgment

This research was sponsored by the Division of Materials Sciences, U.S. Department of Energy, under contract DE-AC05-84OR21400 with Martin Marietta Energy Systems, Inc. The authors would like to thank Dr. H.M. Chung of Argonne National Laboratory for supplying the laboratory-aged CF 8 alloy and K.F. Russell for her assistance in specimen preparation.

REFERENCES

- [1] M.K. Miller, J. Bentley, S.S. Brenner and J.A. Spitznagel, *J. de Physique*, C9, 385 (1984).
- [2] O.K. Chopra and H.M. Chung, Proc. 13th Water Reactor Safety Research Information Meeting, National Bureau of Standards, Gaithersburg, (1985)
- [3] H.M. Chung and O.K. Chopra, Proc. 2nd Int. Symposium on Environmental Degradation of Materials in Nuclear Power Systems - Water Reactors, Monterey, American Nuclear Society, ed. J.T. Roberts, J.R. Weeks and G.J. Theus, p.289 (1985)
- [4] M.K. Miller, *J. de Physique*, C2, 493 (1986); C2, 499 (1986)
- [5] J. Bentley, M.K. Miller, S.S. Brenner and J.A. Spitznagel, Proc. 43rd. Electron Microscopy Society of America, Louisville, ed. G.W. Bailey, p328; (1985)
- [6] F.X. Spiegel, D. Bardos, and P.A. Beck, *Trans. AIME*, 227, 575 (1963)
- [7] J.M. Vitek, *Met. Trans*, in press.
- [8] S.S. Brenner, M.K. Miller and W.A. Soffa, *Scripta Met.*, 16, 831 (1982)
- [9] G. Slama, P. Petrequin, S.H. Masson, and T. Mager, SMIRT Conf. Seminar 6, "Assuring Structural Integrity of Steel Reactor Pressure Boundary Components", Monterey, August 1985.

DISCLAIMER

This report was prepared as an account of work sponsored by an agency of the United States Government. Neither the United States Government nor any agency thereof, nor any of their employees, makes any warranty, express or implied, or assumes any legal liability or responsibility for the accuracy, completeness, or usefulness of any information, apparatus, product, or process disclosed, or represents that its use would not infringe privately owned rights. Reference herein to any specific commercial product, process, or service by trade name, trademark,